Modelling molecular transport in human pial perivasculature

Marius Causemann[†]*, Rami Masri*, Miroslav Kuchta*, & Marie E. Rognes*

*Dept. of Numerical Analysis and Scientific Computing, Simula Research Laboratory

[†]mariusca@simula.no

Modelling molecular transport in the human brain

Molecular transport in perivascular spaces (PVSs) plays a pivotal role in clearance and delivery in the human brain. Previous studies indicate rapid movement of molecules in the subarachnoid space (SAS) and PVSs surrounding pial arteries, but the exact mechanisms and influencing factors remain incompletely understood. Using a one-dimensional network to represent the PVS, embedded within a three-dimensional model of the brain parenchyma and its surrounding cerebrospinal fluid (CSF)-filled space, we construct a comprehensive molecular transport model in the human brain environment (Fig. 1).

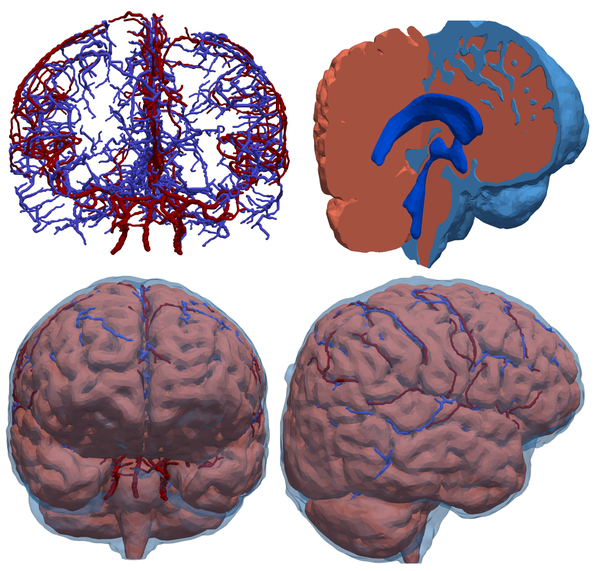

Figure 1: Top: Arterial (red) and venous (blue) networks (left) and the brain tissue (salmon) and CSF space (blue) (right). Bottom: Coronal and sagittal view of the complete model, including the parenchymal tissue, the CSF space, and arterial and venous networks (based on imaging data from [1]).

Multi-dimensional intracranial transport equations

We model diffusion, convection and exchange of a solute in PVSs, the surrounding CSF, and the brain parenchyma via a comprehensive multi-dimensional transport model [4]. More specifically, we solve for a solute concentration c in the CSF space Ω_{CSF} and the parenchymal tissue Ω_{PAR}, and an averaged solute concentration $\hat{c}$ in a 1D network of centerlines Λ representing the PVS, such that the following equations hold

$$\partial_t(\phi c) - \nabla \cdot (D\nabla(\phi c)) + \nabla \cdot (\boldsymbol{u}c) + \xi(\overline{c} - \hat{c})\delta_\Gamma = 0 \quad \text{in} \quad \Omega_{\text{CSF}} \cup \Omega_{\text{PAR}}$$
$$\partial_t(A\phi\hat{c}) - \partial_s(\hat{D}A\partial_s(\phi\hat{c})) + \partial_s(A\hat{u}\hat{c}) + \xi P(\hat{c} - \overline{c}) = 0 \quad \text{in} \quad \Lambda$$

Here ϕ is the fluid volume fraction (or porosity) of the brain (where $\phi \ll 1$), of the SAS (where $\phi = 1$) and of the PVS (where $0 \ll \phi \leq 1$); $D = D_{\text{eff}}(1 + R)$ is the diffusion coefficient accounting for the enhancement of the effective diffusion coefficient D_{eff} by a dispersion factor R; $\boldsymbol{u}$ and $\hat{u}$ are convective velocity fields in Ω and Λ, respectively; ξ is the permeability across the PVS interface; P and A are the perimeter and area of the PVS, respectively; and $\overline{c}$ denotes the lateral average of the concentration over the outer perivascular boundary. Allowing solute transport across the pial surface Γ_{Pia} with a permeability β and enforcing an influx of solute c_{in} via the spinal canal Γ_{SC} over the first two hours, we further impose

$$-D\nabla c_{\text{PAR}} \cdot \boldsymbol{n} = -D\nabla c_{\text{CSF}} \cdot \boldsymbol{n} = \beta(c_{\text{PAR}} - c_{\text{CSF}}) \quad \text{on} \quad \Gamma_{\text{Pia}}$$
$$D\nabla c_{\text{CSF}} \cdot \boldsymbol{n} - c_{\text{CSF}}\boldsymbol{u} \cdot = c_{\text{in}} \max(1 - |t - 1h|, 0) \quad \text{on} \quad \Gamma_{\text{SC}}.$$

Cerebrospinal fluid flow in the subarachnoid space

We consider a steady velocity field resulting from CSF production on the lateral ventricle wall Γ_{LV} and outflow resistance R_0 on the outer boundary Γ_{skull} [2]. We solve the Stokes equations for the velocity u_{CSF} and the pressure p

$$-\mu\Delta\boldsymbol{u}_{\text{CSF}} + \nabla p = 0 \quad \text{in } \Omega_{\text{CSF}},$$
$$\nabla \cdot \boldsymbol{u}_{\text{CSF}} = 0 \quad \text{in } \Omega_{\text{CSF}},$$
$$\mu\nabla\boldsymbol{u}_{\text{CSF}} \cdot \boldsymbol{n} - p\boldsymbol{n} = -R_0(\boldsymbol{u} \cdot \boldsymbol{n})\boldsymbol{n} \quad \text{on } \Gamma_{\text{skull}}$$
$$\boldsymbol{u}_{\text{CSF}} = \boldsymbol{0} \text{ on } \Gamma_{\text{Pia}} \quad \text{and} \quad \boldsymbol{u}_{\text{CSF}} = u_{\text{prod}} \cdot \boldsymbol{n} \quad \text{on } \Gamma_{\text{LV}}.$$

Similarly, we compute a cardiac-driven flow field at peak vascular expansion and derive the diffusion enhancement factor R following the theory of pulsatile mixing [3] (Fig. 2).

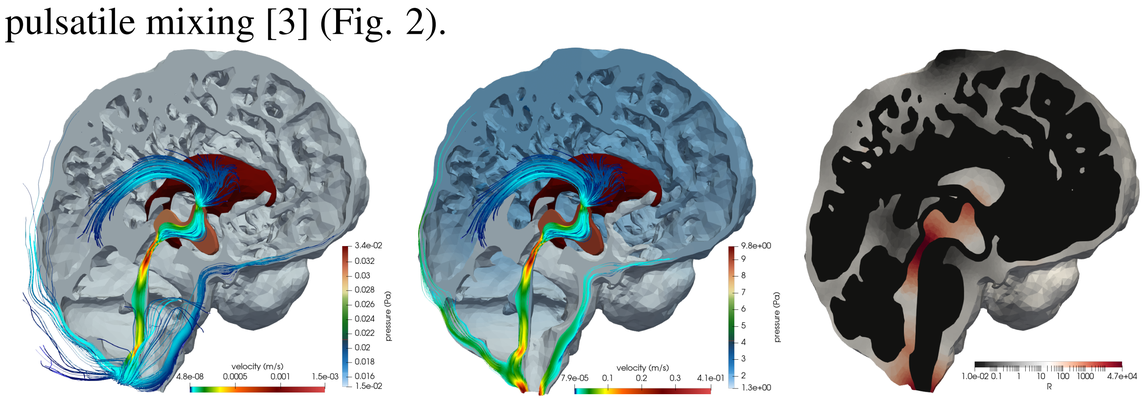

Figure 2: left: CSF flow field driven by CSF production (630 ml/day across the lateral ventricle (LV) walls); middle: cardiac-driven CSF flow at peak arterial expansion (2 ml/s and 10 ml/s across the LV walls and the pia, respectively); right: diffusion enhancement factor R due to dispersive mixing driven by cardiac pulsatility.

Advective CSF flow drives tracer transport

Investigating the contribution of the advective velocity field resulting from CSF production, we compare the advective model with a purely diffusive transport model and find a substantial increase in tracer spreading over the first 24 hours. Specifically, the velocity field advects the tracer towards the upper convexity of the skull, whereas purely diffusive transport confines the tracer to ventral brain regions and the ventricular system (Fig. 3).

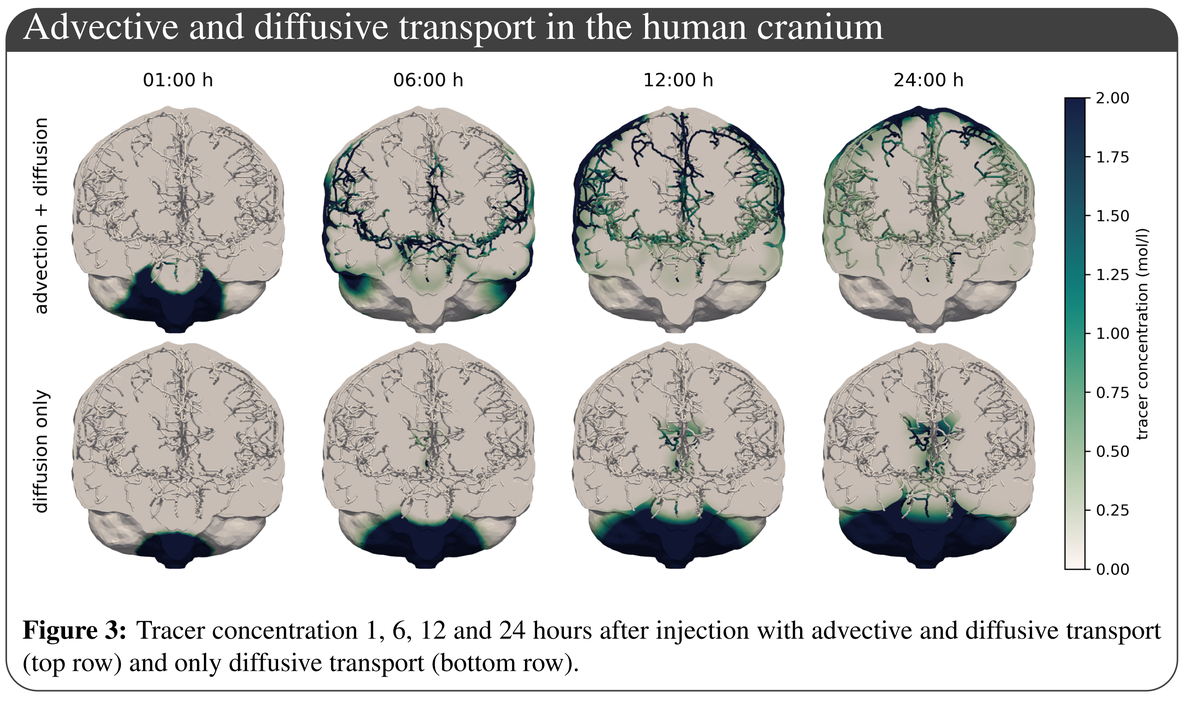

Figure 3: Tracer concentration 1, 6, 12 and 24 hours after injection with advective and diffusive transport (top row) and only diffusive transport (bottom row).

For both models, a major share of injected tracers remains in the CSF space over the first 24 hours. However, we observe a larger crossover into the parenchymal tissue and PVS spaces for the advective model (Fig. 4).

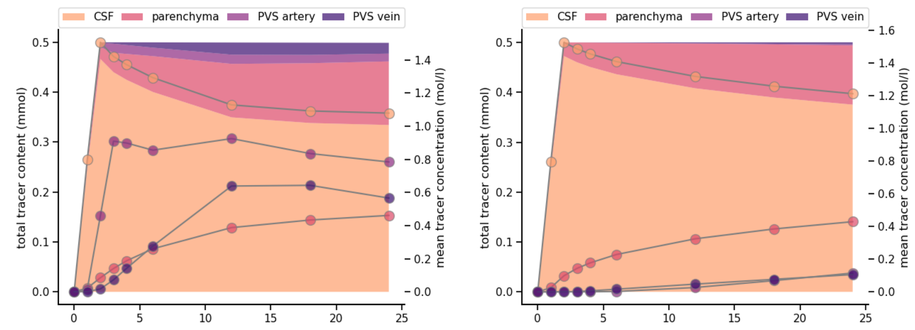

Figure 4: Total tracer content and concentration in CSF, parenchyma, arterial PVS and venous PVS with advective and diffusive (left) and only diffusive transport (right).

Compartmentalization of the subarachnoid space

We investigate the effect of perivascular ensheathment of arteries in the SAS by varying the PVS-CSF permeability from a substantial barrier ($\xi = 3.7 \cdot 10^{-7}\,\text{m}^2/\text{s}$) to a more continuous representation ($\xi_{\text{cont}} = 10\xi$) (Fig. 5). The relative difference in tracer concentration in the arterial PVS $\hat{c}$ and its surrounding space $\overline{c}$ defined as $\Delta_{c_{\text{rel}}} := (\overline{c} - \hat{c})/\overline{c}$ substantially decreases with the increase of permeability, especially during the first hours after injection.

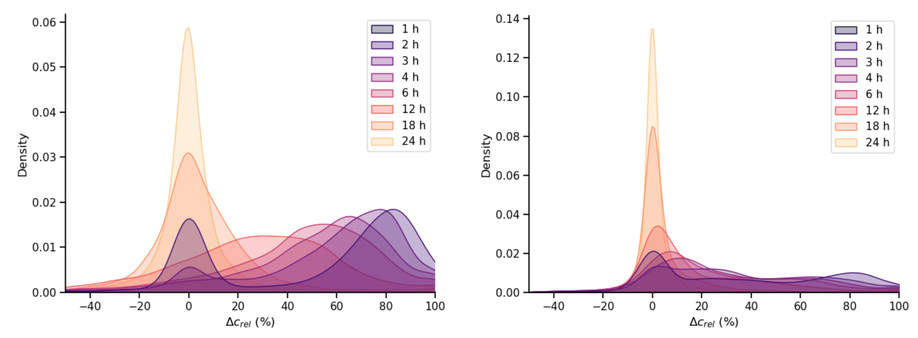

Figure 5: Distribution of the relative difference in tracer concentration in the arterial PVS and the surrounding space (left) compared with a tenfold increased PVS-CSF permeability (right).

Future work

We will extend the baseline model to account for various convective flow mechanisms in the PVS spaces and the parenchyma, and investigate physiological alterations associated with sleep and pathological states.

References

[1] E. Hodneland, E. Hanson, O. Sævareid, G. Nævdal, A. Lundervold, V. Šoltészová, A. Z. Munthe-Kaas, A. Deistung, J. R. Reichenbach, and J. M. Nordbotten. A new framework for assessing subject-specific whole brain circulation and perfusion using mri-based measurements and a multi-scale continuous flow model. *PLoS computational biology*, 15(6):e1007073, 2019.

[2] M. Hornkjøl, L. Valnes, G. Ringstad, M. Rognes, P. Eide, K. Mardal, and V. Vinje. CSF circulation and dispersion yield rapid clearance from intracranial compartments. *Frontiers in Bioengineering and Biotechnology*, 10:932469–932469, 2022.

[3] M. Keith Sharp, R. O. Carare, and B. A. Martin. Dispersion in porous media in oscillatory flow between flat plates: applications to intrathecal, periarterial and paraarterial solute transport in the central nervous system. *Fluids and Barriers of the CNS*, 16:1–17, 2019.

[4] R. Masri, M. Zeinhofer, M. Kuchta, and M. Rognes. The modelling error in multi-dimensional time-dependent solute transport models. *arXiv*, 2023.

We acknowledge support from the Research Council of Norway via FRIPRO grant #324239 (EMIx) and from the national infrastructure for computational science in Norway, Sigma2, via grant #NN8049K.